Available online at http://scik.org
Commun. Math. Biol. Neurosci. 2022, 2022:90
https://doi.org/10.28919/cmbn/7638
ISSN: 2052-2541

THE INFLUENCE OF FEAR ON THE DYNAMIC OF AN ECO-EPIDEMIOLOGICAL SYSTEM WITH PREDATOR SUBJECT TO THE WEAK ALLEE EFFECT AND HARVESTING

ZINAH KHALID MAHMOOD, HUDA ABDUL SATAR*

Department of Mathematics, College of Science, University of Baghdad, Baghdad 10071, IRAQ.

Copyright © 2022 the author(s). This is an open access article distributed under the Creative Commons Attribution License, which permits unrestricted use, distribution, and reproduction in any medium, provided the original work is properly cited.

Abstract: In this paper, an eco-epidemiological prey-predator system when the predator is subjected to the weak Allee effect, and harvesting was proposed and studied. The set of ordinary differential equations that simulate the system's dynamic is constructed. The impact of fear and Allee's effect on the system's dynamic behavior is one of our main objectives. The properties of the solution of the system were studied. All possible equilibrium points were determined, and their local, as well as global stabilities, were investigated. The possibility of the occurrence of local bifurcation was studied. Numerical simulation was used to further evaluate the global dynamics and understood the effects of varying parameters on the asymptotic behavior of the system. It is observed that the system has different types of attractors including stable point, periodic, and even bi-stable behavior.

Keywords: prey-predator; fear; Allee effect, harvesting, bi-stability; bifurcation.

2010 AMS Subject Classification: 92D25, 92D30, 34D20, 37G10.

*Corresponding author
E-mail address: huda.oun@sc.uobaghdad.edu.iq
Received July 30, 2022

1. INTRODUCTION

The study of eco-epidemiological systems is important to obtain better real-world life due to their direct effects on the capability of the environment. Since mathematical modeling can be used to simulate the dynamical behavior of these biological systems and conclude all the requirements to improve human life, hence the mathematical models in eco-epidemiology are extensively used to understand and solve a lot of real-world life problems. The first eco-epidemiological model including infectious disease in the prey was introduced by Anderson and May [1]. Later on, a number of researchers proposed and studied eco-epidemiological models involving many biological factors [2-13].

Many species suffer from Allee effects, disease, and predation. For instance, the combined impact of disease and the Allee effect has been observed in the African wild dog Lycaon pictus [14, 15] and the island fox Urocyon littoralis [16, 17]. Both the African wild dog and island fox should have their enemies in the wild. Thus, understanding the combined impact of Allee effects and disease on population dynamics of predator-prey interactions can help us have better insights on species abundance as well as the outbreak of disease. Therefore, we can make better policies to regulate the population and disease. Thus, for the first time, we propose a general predator-prey model with Allee effects and disease in prey to investigate how the interplay of Allee effects and disease in prey affect the population dynamics of both prey and predator.

Although there are many studies interested in eco-epidemiology in literature, the impact of the Allee effect on eco-epidemiological systems is not taken sufficient studies yet. The Allee effect named after Allee [11]. Biswas et al [18] considered a system of delay differential equations that represent prey-predator eco-epidemic dynamics with a weak Allee effect in the growth of the predator population. Recently, Huda Abdul Satar studied the dynamics of an eco-epidemiological model with the Allee effect and harvesting in the predator [19].

Also, several field data and experiments on terrestrial vertebrates exhibited that the fear of predators would cause a substantial variability of prey demography. Fear of predator population enhances the survival probability of the prey population, and it can greatly reduce the reproduction of the prey population. Based on the experimental evidence [20].

Moreover, the impact of harvesting of a particular species on the dynamic behavior of the food chain and food web is also investigated. In fact, the existence of harvesting on some interacting species is beneficial from both ecological as well as economic points of view. Several studies of the effect of harvesting of one species on the other have been done using different types of harvesting functions since the pioneering work by Clark [21]. Therefore, in this paper, we intend to study the influence of fear on an eco-epidemiological system when the predators are subject to the weak Allee effect and harvesting.

2. THE MODEL FORMULATION

In this section, a mathematical modeling approach was used to study the role of fear and the Allee effect on the dynamical behavior of the harvested prey-predator system. In order to formulate the model, the following assumptions are adopted.

It is assumed that the prey species is contracted the SI type of infectious disease, therefore the prey species is divided into two compartments: susceptible prey that is denoted to their population size at time t by $S(t)$, and the second compartment contains the infected prey, which is denoted to their population size at time t by $I(t)$.

The prey species grows logistically in the absence of the predator where the infected prey cannot reproduce while it has the capability to compete with the other prey species to reach the environment carrying capacity. Furthermore, the disease causes extra death for the infected prey.

The prey reproduction is affected by the fear due to the existence of predation.

The predator species, which represents their population size at time t by $P(t)$, consumes both the prey according to the Lottka-Volttera functional response and decays exponentially in the absence of food. Further, it is assumed that the predator is affected by the weak Allee effect and harvesting.

Accordingly, the dynamics of the above-described eco-epidemiological system can be represented by using the following differential equations:

$$\begin{aligned}
\frac{dS}{dt} &= S\left[\frac{r}{1+kP} - b\,(S+I) - \beta I - aP\right] = Sg_1(S,I,P),\\
\frac{dI}{dt} &= I\,[\,\beta S - aP - d_1\,] = Ig_2(S,I,P), \qquad , \qquad (1)\\
\frac{dP}{dt} &= P\left[a\,(\alpha S + \gamma I)\,\frac{P}{\theta+P} - d_2 - qE\right] = Pg_3(S,I,P),
\end{aligned}$$

where $S(t) \geq 0,\ I(t) \geq 0,$ and $P(t) \geq 0$. All parameters are assumed to be positive and described in Table (1).

Moreover, the functions $g_i = 1,2,3$ in the right-hand side of the system (1) are continuous and have continuous partial derivatives in the following space.

$$\mathfrak{L} = \{(S,I,P) \in \mathbb{R}^3 : S(0) \geq 0, I(0) \geq 0, P(0) \geq 0\}$$

Therefore, the system (1) solution exists and is unique.

Table (1) Brief description of the system (1) parameters:

Parameter	Descriptions
r	The intrinsic growth rate of the susceptible prey.
$b \in (0,1)$	The intraspecific competition of the prey (Susceptible and infected).
$\beta \in (0,1)$	The infection rate.
a	The attack rate of the prey by a predator.
k	The fear rate.
$d_1 \in (0,1)$	The disease death rate of the infected prey.
$d_2 \in (0,1)$	The natural death rate of predators.
$\alpha \in (0,1)$	The conversion rate of the susceptible prey to the predator.
$\gamma \in (0,1)$	The conversion rate infected prey to the predator.
θ	The Allee effect rate.
q, E	The harvesting catchability constant and the effort rate.

Theorem 1. All solutions of system (1) initiating in $\mathfrak{L}$ are uniformly bounded.

Proof. From the first equation of system (1), the following is obtained $\frac{dS}{dt} \leq (r - bS)S$. It is simple to verify that $S \leq \frac{r}{b}$ for $t \to \infty$.

Now, define the function $\omega_1(t) = S(t) + I(t) + P(t)$, then after some algebraic manipulation we have:

$$\frac{d\omega_1}{dt} \leq rS - d_1 I - (d_2 + qE)P.$$

Then, it is obtained that $\frac{d\omega_1}{dt} \leq 2rs - M\omega_1$, where $M = min\,\{r, d_1, (d_2 + qE)\}$. Therefore, an application of Gronwall inequality [22], gives that $\omega_1 \leq \frac{2r^2}{Mb} = \mu$. Hence, all solutions are uniformly bounded in $\mathfrak{L}$.

3. Existence of Equilibrium Points and Their Local Stability Analysis

The existence of equilibrium points (EPs) of the system (1) is carried out. There are at most five non-negative EPs of the system (1), these points are described as follows:

- The Vanishing equilibrium point (VEP) that is denoted by $E_0 = (0,0,0)$ always exists.
- The axial equilibrium point (AXEP) that is denoted by $E_1 = \left(\frac{r}{b}, 0, 0\right)$ always exists.
- The predator-free equilibrium point (PFEP) is denoted by $E_2 = (\hat{S}, \hat{I}, 0)$ where

$$\hat{S} = \frac{d_1}{\beta}, \hat{I} = \frac{r\beta - bd_1}{\beta(b+\beta)}. \tag{2}$$

Clearly, the PFEP exists uniquely in the $xy-$plane under the following condition:

$$d_1 < \frac{r\beta}{b}. \tag{3}$$

- The disease-free equilibrium point (DFEP) is denoted by $E_3 = (\bar{S}, 0, \bar{P})$ where

$$\bar{P} = \frac{(d_2+qE)\theta}{a\,\alpha\bar{S} - (d_2+qE)}, \tag{4a}$$

while $\bar{S}$ represents a positive root for the cubic polynomial equation:

$$A_1 S^3 + A_2 S^2 + A_3 S + A_4 = 0 \tag{4b}$$

where

$$A_1 = -b\,a^2\alpha^2,$$

$$A_2 = r\,a^2\alpha^2 + 2a\,\alpha b(d_2 + qE) - kba\alpha\theta\,(d_2 + qE),$$

$$A_3 = (d_2 + qE)[-2a\alpha r - b\,(d_2 + qE) + kb\theta(d_2 + qE) - a^2\alpha\theta],$$

$$A_4 = (d_2 + qE)^2\,(r + a\theta - ka\,\theta^2).$$

Clearly, the DFEP exists uniquely on the $SP-$axis under conditions

$$\frac{(d_2+qE)}{a\alpha} < \bar{S} \tag{5a}$$

$$k < \frac{r+a\theta}{a\,\theta^2}, \tag{5b}$$

with one of the following two conditions:

$$\left.\begin{array}{c} r\,a^2\alpha^2 + 2a\,\alpha b(\,d_2 + qE) < kba\alpha\theta\,(d_2 + qE) \\ 2a\alpha r + b\,(d_2 + qE) + a^2\alpha\theta < kb\theta(d_2 + qE) \end{array}\right\}. \tag{5c}$$

• The positive equilibrium point (PEP) is denoted by $E_4 = (\,\bar{\bar{S}}, \bar{\bar{I}}, \bar{\bar{P}}\,)$ where

$$\bar{\bar{S}} = \frac{a\bar{\bar{P}}+d_1}{\beta} \text{ and } \bar{\bar{I}} = \frac{r\beta-[b(a\bar{\bar{P}}+d_1)+a\bar{\bar{P}}](1+k\bar{\bar{P}})}{\beta(1+k\bar{\bar{P}})(\beta+b)}, \tag{6a}$$

while $\bar{\bar{P}}$ represents a positive root for the cubic polynomial equation:

$$B_1P^3 + B_2P^2 + B_3P + B_4 = 0 \tag{6b}$$

where:

$$\begin{aligned} B_1 &= a^2K[(\alpha-\gamma)b + \alpha\beta + \gamma], \\ B_2 &= a^2\alpha(\beta+b) + a\alpha d_1k(\beta+b) - [a\gamma(a(1+b) + bk\,d_1)] \\ &\qquad -\beta k(d_2+qE)\,(\beta+b), \\ B_3 &= a\alpha d_1(\beta+b) + a\gamma(r\beta - b\,d_1) - \beta\theta k(\beta+b)(d_2+qE) \\ &\qquad -\beta(\beta+b)(d_2+qE), \\ B_4 &= -\beta\theta\,(\beta+b\,)(d_2+qE) < 0. \end{aligned}$$

Clearly, the PEP exists uniquely under conditions:

$$\left[b\left(a\bar{\bar{P}} + d_1\right) + a\bar{\bar{P}}\right]\left(1 + k\bar{\bar{P}}\right) < r\beta, \tag{7a}$$

$$\gamma b < \alpha(b+\beta) + \gamma, \tag{7b}$$

with one of the following two conditions:

$$\left.\begin{array}{c} [a\gamma(a(1+b) + bk\,d_1)] + \beta k(d_2+qE)\,(\beta+b) < a\alpha(\beta+b)(a+d_1k) \\ a\alpha d_1(\beta+b) + a\gamma(r\beta - b\,d_1) < \beta(\beta+b)(d_2+qE)[\theta k+1] \end{array}\right\}. \tag{7c}$$

Now, to establish the local dynamics behaviors of the system (1), around each of these EPs, the Jacobian matrix (JM) is computed, and then compute the eigenvalues for the resulting matrix.

$$J(S,I,P) = \begin{bmatrix} S\frac{\partial g_1}{\partial S} + g_1 & S\frac{\partial g_1}{\partial I} & S\frac{\partial g_1}{\partial P} \\ I\frac{\partial g_2}{\partial S} & I\frac{\partial g_2}{\partial I} + g_2 & I\frac{\partial g_2}{\partial P} \\ P\frac{\partial g_3}{\partial S} & P\frac{\partial g_3}{\partial I} & P\frac{\partial g_3}{\partial P} + g_3 \end{bmatrix}, \tag{8}$$

where:

$$\frac{\partial g_1}{\partial S} = -b,\ \frac{\partial g_1}{\partial I} = -(b+\beta),\ \frac{\partial g_1}{\partial P} = -\left(\frac{rk}{(1+kP)^2} + a\right),$$

$$\frac{\partial g_2}{\partial S} = \beta,\ \frac{\partial g_2}{\partial I} = 0,\ \frac{\partial g_2}{\partial P} = -a,\ \frac{\partial g_3}{\partial S} = \frac{a\alpha P}{\theta+P},\ \frac{\partial g_3}{\partial I} = \frac{a\gamma P}{\theta+P},\ \frac{\partial g_3}{\partial P} = a(\alpha S + \gamma I)\frac{\theta}{(\theta+P)^2}.$$

Therefore, the JM at VEP can be written as

$$J_{VEP} = \begin{bmatrix} r & 0 & 0 \\ 0 & -d_1 & 0 \\ 0 & 0 & -(d_2+qE) \end{bmatrix} \tag{9}$$

Clearly, the eigenvalues are $\lambda_{01} = r, \lambda_{02} = -d_1,$ and $\lambda_{03} = -(d_2+qE)$. Thus the VEP is a saddle point.

The JM at AXEP can be written as:

$$J_{AXEP} = \begin{bmatrix} -r & -\left(r+\frac{\beta r}{b}\right) & -\left(\frac{r^2k+ra}{b}\right) \\ 0 & \frac{\beta r}{b} - d_1 & 0 \\ 0 & 0 & -(d_2+qE) \end{bmatrix} \tag{10}$$

Here the eigenvalues are $\lambda_{11} = -r < 0,\ \lambda_{12} = \frac{\beta r}{d} - d_1,\ \lambda_{13} = -(d_2+qE) < 0$. Therefore, the AXEP is locally asymptotically stable (LAS) if and only if the following condition holds:

$$\frac{\beta r}{b} < d_1 \tag{11}$$

The JM at PFEP can be written as:

$$J_{PFEP} = \begin{bmatrix} -b\,\hat{S} & -(b+\beta)\hat{S} & -(rk+a)\hat{S} \\ \beta\hat{I} & 0 & -a\hat{I} \\ 0 & 0 & -(d_2+qE) \end{bmatrix} \tag{12}$$

Therefore, the characteristic equation of J_{PFEP} can be determined as follows:

$$(\lambda^2 - T_1\lambda + D_1)[-(d_2+qE) - \lambda] = 0, \tag{13a}$$

where $T_1 = -b\,\hat{S} < 0$ and $D_1 = (b+\beta)\beta\hat{S}\hat{I} > 0$. Hence, the eigenvalues of J_{PFEP} are given by:

$$\lambda_{21} = \frac{T_1}{2} + \frac{1}{2}\sqrt{{T_1}^2 - 4D_1},\ \lambda_{22} = \frac{T_1}{2} - \frac{1}{2}\sqrt{{T_1}^2 - 4D_1},\ \lambda_{23} = -(d_2+qE). \tag{13b}$$

Therefore the PFEP is unconditionally LAS whenever it exists.

The JM at the DFEP can be written as:

$$J_{DFEP} = \begin{bmatrix} -b\bar{S} & -(b+\beta)\bar{S} & -\left(\frac{rk}{(1+k\bar{P})^2} + a\right)\bar{S} \\ 0 & \beta\bar{S} - a\bar{P} - d_1 & 0 \\ \frac{a\alpha}{\theta+\bar{P}}\bar{P}^2 & \frac{a\gamma}{\theta+\bar{P}}\bar{P}^2 & \frac{a\alpha\theta\bar{S}\bar{P}}{(\theta+\bar{P})^2} \end{bmatrix} \tag{14}$$

Therefore, the characteristic equation of J_{DFEP} is given by:

$$(\lambda^2 - T_2\,\lambda + D_2)[\beta\bar{S} - a\bar{P} - d_1 - \lambda] = 0, \tag{15a}$$

where $T_2 = -b\bar{S} + \frac{a\alpha\theta\bar{S}\bar{P}}{(\theta+\bar{P})^2}$, and $D_2 = -\left(\frac{ba\alpha\theta\bar{S}^2\,\bar{P}}{(\theta+\bar{P})^2}\right) + \left[\frac{rk}{(1+k\bar{P})^2} + a\right]\frac{a\alpha}{\theta+\bar{P}}\bar{S}\bar{P}^2$.

Then the eigenvalues of J_{DFEP} are given by:

$$\lambda_{31} = \frac{T_2}{2} + \frac{1}{2}\sqrt{{T_2}^2 - 4D_2},\ \lambda_{32} = \beta\bar{S} - a\bar{P} - d_1,\ \lambda_{33} = \frac{T_2}{2} - \frac{1}{2}\sqrt{{T_2}^2 - 4D_2}. \tag{15b}$$

Then the DFEP is LAS if and only if the following conditions hold.

$$\frac{a\alpha\theta\bar{P}}{(\theta+\bar{P})^2} < b, \tag{16a}$$

$$\frac{b\theta\bar{S}}{\theta+\bar{P}} < \left(\frac{rk}{(1+k\bar{P})^2} + a\right)\bar{P}, \tag{16b}$$

$$\beta\bar{S} < a\bar{P} + d_1. \tag{16c}$$

Finally, the local stability conditions for the PEP are established in the following theorem.

Theorem 2. The PEP of the system (1) is a LAS if and only if the following conditions are satisfied.

$$a\left(\alpha\bar{\bar{S}} + \gamma\bar{\bar{I}}\right)\frac{\theta\bar{\bar{P}}}{(\theta+\bar{\bar{P}})^2} < b\bar{\bar{S}}, \tag{17a}$$

$$h_{32}(h_{13}h_{21} - h_{11}h_{23}) < h_{12}(h_{21}h_{33} - h_{23}h_{31}), \tag{17b}$$

$$h_{11}h_{33} - h_{13}h_{31} > 0, \tag{17c}$$

$$h_{12}(h_{11}h_{21} + h_{23}h_{31}) + h_{32}(h_{23}h_{33} + h_{13}h_{21}) > 0, \tag{17d}$$

where all the new symbols are given in the proof.

Proof. Direct computation shows that the JM at the PEP is determined as

$$J_{PEP} = \begin{bmatrix} -b\bar{\bar{S}} & -(b+\beta)\bar{\bar{S}} & -\left(\frac{rk}{(1+k\bar{\bar{P}})^2} + a\right)\bar{\bar{S}} \\ \beta\bar{\bar{I}} & 0 & -a\bar{\bar{I}} \\ \frac{a\alpha\bar{\bar{P}}^2}{\theta+\bar{\bar{P}}} & \frac{a\gamma\bar{\bar{P}}^2}{\theta+\bar{\bar{P}}} & a\left(\alpha\bar{\bar{S}} + \gamma\bar{\bar{I}}\right)\frac{\theta\bar{\bar{P}}}{(\theta+\bar{\bar{P}})^2} \end{bmatrix} = (h_{ij}). \tag{18}$$

Therefore, the characteristic equation of J_{PEP} can be determined as

$$\lambda^3 + \delta_1\lambda^2 + \delta_2\lambda + \delta_3 = 0, \tag{19}$$

where

$$\begin{aligned} \delta_1 &= -(h_{11} + h_{33}), \\ \delta_2 &= -h_{12}h_{21} - h_{23}h_{32} + h_{11}h_{33} - h_{13}h_{31}, \\ \delta_3 &= -[h_{32}(h_{13}h_{21} - h_{11}h_{23}) - h_{12}(h_{21}h_{33} - h_{23}h_{31})]. \end{aligned}$$

while

$$\Delta = \delta_1\delta_2 - \delta_3 = \delta_1(h_{11}h_{33} - h_{13}h_{31}) + h_{12}(h_{11}h_{21} + h_{23}h_{31}) + h_{32}(h_{23}h_{33} + h_{13}h_{21})$$

Now, the proof follows if all the eigenvalues of J_{PEP} have negative real parts, which are satisfied if and only if $\delta_i > 0, (i = 1,3)$, and $\Delta > 0$ [23], straightforward computation shows that the conditions (17a)-(17d) guarantee the satisfying of these requirements. Then, the PEP is LAS if the conditions (17a)-(17d) hold.

In following, the persistence of system (1) is discussed. Persistence means biologically that the survival of all the species for all time. While it is means the solution has no omega limit set in the boundary planes of the state space $\mathfrak{L}$ mathematically.

Now according to the system (1) in the absence of the disease then the following subsystem is obtained

$$\begin{aligned} \frac{dS}{dt} &= S\left[\frac{r}{1+kP} - bS - aP\right] = Sg_{11}(S,P), \\ \frac{dP}{dt} &= P\left[\frac{a\,\alpha S\,P}{\theta+P} - d_2 - qE\right] = Pg_{22}(S,P). \end{aligned} \tag{20}$$

The subsystem (20) is a $2D$ system that has a unique positive point given by $(\bar{S},\bar{P})$, which are given by equations (4a)-(4b) and exists uniquely in the SP −plane under the conditions (5a)-(5c). According to the well-known Poincare Bendixon theorem, the solution of the bounded system (20) approaches either the EP. $(\bar{S},\bar{P})$, or else to the periodic dynamics. Now by using the continuous $\pi_1 = \frac{1}{SP}$, it is obtained that:

$$\nabla = \frac{\partial}{\partial S}(\pi_1 S g_{11}) + \frac{\partial}{\partial P}(\pi_1 P g_{22}) = -\frac{b}{P} + \frac{a\,\alpha\,\theta}{(\theta+P)^2}.$$

Therefore, according to the Dulac-Bendixon criterion [24], the subsystem (20) has no periodic dynamics in the interior of the positive quadrant of the SP −plane if one of the following conditions are met.

$$\left.\begin{aligned} \frac{a\,\alpha\,\theta}{(\theta+P)^2} &< \frac{b}{P} \\ \frac{b}{P} &< \frac{a\,\alpha\,\theta}{(\theta+P)^2} \end{aligned}\right\}. \tag{21}$$

Consequently, due to Poincare Bendixon's theorem, the equilibrium point $(\bar{S},\bar{P})$ is a GAS whenever it exists. Hence system (1) has no periodic dynamics in the boundary SP −planes under condition (21).

Theorem 3. If the following conditions, with the condition (21), are met then system (1) is uniformly persistent.

$$r\beta < d_1 < \frac{\beta r}{b}. \tag{22a}$$

$$a\bar{P} + d_1 < \beta\bar{S}. \tag{22b}$$

Proof: Define the following function using the average Lyapunov function method [25]. $\pi_2(S,I,P) = S^{n_1}I^{n_2}P^{n_3}$, where $n_i, \forall i = 1,2,3$ represent the positive constants. Thus, $\pi_2(S,I,P) > 0$, for all $(S,I,P) \in int.\mathfrak{L}$ and $\pi_2(S,I,P) \to 0$ when any of their variables gets close to zero. Therefore, it is gained that

$$\sigma(S,I,P) = \frac{\pi_2'(S,I,P)}{\pi_2(S,I,P)} = n_1\left[\frac{r}{1+kP} - b\,(\,S + I\,) - \,\beta I - aP\,\right]$$
$$+n_2[\,\beta S - aP - d_1\,] + \,n_3\left[\,a\,(\,\alpha S + \,\gamma I\,)\,\frac{P}{\theta+P} - \,d_2 - qE\,\right].$$

Recall that, according to condition (21) there is no periodic dynamics in the interior of SP −plane and hence the only attracting set in the interior of SP −plane is the DFEP, and condition (22a) guarantees that the PFEP does not exist and hence due to the index theory there are no periodic dynamics in the interior of SI −plane.

Now, the proof is done using the average Lyapunov function if $\sigma(E) > 0$ for every attractor point E on the border planes. Moreover, since

$$\sigma(E_0) = n_1 r - n_2 d_1 - n_3(\,d_2 + qE\,),$$

$$\sigma(E_1) = n_2\left(\beta\frac{r}{b} - d_1\right) - \,n_3(\,d_2 + qE),$$

$$\sigma(E_3) = n_2[\,\beta\bar{S} - a\bar{P} - d_1\,].$$

Thus, choosing $n_1 > n_2 > n_3 > 0$ as a sufficiently needed with the help of condition (22a) leads to $\sigma(E_0) > 0$ and $\sigma(E_2) > 0$. However, $\sigma(E_3) > 0$ due to condition (22b). Thus the proof is done.

4. GLOBAL STABILITY ANALYSIS

In this section, the global dynamics of the system (1) or else the basin of attraction for each EPs are investigated using Lyapunov functions, as demonstrated in the next theorems

Theorem 4. Suppose that the AXEP is LAS, then it is a GAS if the following sufficient conditions are satisfied:

$$(b+\beta)\tilde{S} < d_1 \tag{23a}$$

$$(a+rk)\tilde{S} < (d_2+qE) \tag{23b}$$

where $\tilde{S} = \frac{r}{b}$.

Proof. Define ϑ_1 as a real-valued function that is given by

$$\vartheta_1 = \left(S - \tilde{S} - \tilde{S}\ \ln\frac{S}{\tilde{S}}\right) + I + P.$$

It is clear that ϑ_1 is a positive definite function that is defined for all $\{(S,I,P) \in \mathfrak{L}: S > 0, I \geq 0, P \geq 0\}$. Recall that, according to the LAS of the AXEP that is given by equation (11), the PFEP is not exist.

Now by differentiating ϑ_1 with respect to (w.r.t.) time, and then simplify the result, it is obtain that

$$\frac{d\vartheta_1}{dt} \leq -b\left(S-\tilde{S}\right)^2 - \left[d_1 - (b+\beta)\tilde{S}\right]I - \left[(d_2+qE) - (a+rk)\tilde{S}\right]P$$
$$-a(1-\alpha)SP - a(1-\gamma)IP.$$

Using the biological fact that $\boldsymbol{\alpha} \in (\mathbf{0},\mathbf{1})$ and $\boldsymbol{\gamma} \in (\mathbf{0},\mathbf{1})$. It is obtained that

$$\frac{d\vartheta_1}{dt} < -b\left(S-\tilde{S}\right)^2 - \left[d_1 - (b+\beta)\tilde{S}\right]I - \left[(d_2+qE) - (a+rk)\tilde{S}\right]P$$

Consequently, $\frac{d\vartheta_1}{dt}$ is negative definite under the conditions (23a) and (23b). Moreover, since the function ϑ_1 is radially unbounded then the AXEP is a GAS.

Theorem 5. Suppose that the PFEP exists, then it has a basin of attraction that satisfies the following sufficient conditions.

$$a\left(\hat{I}+\hat{S}\right) + rk\hat{S} < (d_2+qE), \tag{24a}$$

$$b\left(I-\hat{I}\right)^2 < \mathcal{M}_1 + \mathcal{M}_2, \tag{24b}$$

here $\mathcal{M}_1 = b\left[\left(S-\hat{S}\right) + \left(I-\hat{I}\right)\right]^2$ and $\mathcal{M}_2 = \left[(d_2+qE) - a\left(\hat{S}+\hat{I}\right) - rk\hat{S}\right]P$.

Proof. Define ϑ_2 as a real-valued function that is given by

$$\vartheta_2 = \left(S - \hat{S} - \hat{S}\ \ln\frac{S}{\hat{S}}\right) + \left(I - \hat{I} - \hat{I}\ln\frac{I}{\hat{I}}\right) + P.$$

It is clear that ϑ_2 is a positive definite function that is defined for all $\{(S,I,P)\in\mathfrak{L}: S>0, I>0, P\geq 0\}$. Now by differentiating ϑ_2 w.r.t. time, and then simplifying the result, it is obtained that

$$\frac{d\vartheta_2}{dt}<-b\big(S-\hat{S}\big)^2-b\big(S-\hat{S}\big)\big(I-\hat{I}\big)-\big[(d_2+qE)-a\big(\hat{I}+\hat{S}\big)-rk\hat{S}\big]P.$$

Additional operations to complete the square are produced.

$$\frac{d\vartheta_2}{dt}<-b\left[\big(S-\hat{S}\big)+\big(I-\hat{I}\big)\right]^2-\left[(d_2+qE)-a\big(\hat{S}+\hat{I}\big)-rk\hat{S}\right]P+b\big(I-\hat{I}\big)^2.$$

Therefore, the derivative $\frac{d\vartheta_2}{dt}$ is negative definite under the conditions (24a) and (24b). Moreover, since the function ϑ_2 is radially unbounded then all the solutions, which are initiated in the interior of the sub-region of $\mathfrak{L}$ and satisfy the conditions (24a) and (24b), are approached asymptotically to PFEP. Hence the proof is done.

Theorem 6. Suppose that the DFEP is LAS, then it has a basin of attraction that satisfies the following sufficient conditions.

$$(b+\beta)\bar{S}<d_1, \tag{25a}$$

$$\left[\frac{rk}{(1+kP)(1+k\bar{P})}+a-\frac{a\alpha P}{\theta+P}\right]^2<\frac{4ba\alpha\bar{S}}{\bar{R}}, \tag{25b}$$

$$\frac{2a\alpha\bar{S}}{\bar{R}}(P-\bar{P})^2<\aleph_1+\aleph_2 \tag{25c}$$

where $\aleph_1=\left[\sqrt{b}(S-\bar{S})+\sqrt{\frac{a\alpha\bar{S}}{\theta+\bar{P}}}(P-\bar{P})\right]^2$, and $\aleph_2=[d_1-(b+\beta)\bar{S}]I$.

Proof. Define ϑ_3 as a real-valued function that is given by

$$\vartheta_3=\left(S-\bar{S}-\bar{S}\ln\frac{S}{\bar{S}}\right)+I+\left(P-\bar{P}-\bar{P}\ln\frac{P}{\bar{P}}\right)$$

It is clear that ϑ_3 is a positive definite function that is defined for all $\{(S,I,P)\in\mathfrak{L}: S>0, I\geq 0, P>0\}$. Now by differentiating ϑ_2 w.r.t. time, and then simplifying the result, it is obtained that

$$\frac{d\vartheta_3}{dt}<-b(S-\bar{S})^2-\left[\frac{rk}{(1+kP)(1+k\bar{P})}+a-\frac{a\alpha P}{\theta+P}\right](S-\bar{S})(P-\bar{P})$$
$$+\frac{a\alpha\bar{S}}{\theta+\bar{P}}(P-\bar{P})^2-[d_1-(b+\beta)\bar{S}]I.$$

Additional operations to complete the square are produced.

$$\frac{d\vartheta_3}{dt}<-\aleph_1-\aleph_2+\frac{2a\alpha\bar{S}}{\bar{R}}(P-\bar{P})^2.$$

Therefore, the derivative $\frac{d\vartheta_3}{dt}$ is negative definite under the conditions (25a) and (25c). Moreover, since the function ϑ_3 is radially unbounded then all the solutions, which are initiated in the interior of the sub-region of $\mathfrak{L}$ and satisfy the conditions (25a), (25b), and (25c) are approached asymptotically to DFEP. Hence the proof is done.

Theorem 7. Suppose that the PEP is LAS, then then it has a basin of attraction that satisfies the following sufficient conditions.

$$\max\left\{\left[\frac{rk}{(1+kP)(1+k\bar{\bar{P}})}+a-\frac{a\alpha P}{\theta+P}\right]^2,\left[a-\frac{a\gamma P}{\theta+P}\right]^2\right\}<\frac{ab(\alpha\bar{\bar{S}}+\gamma\bar{\bar{I}})}{\theta+\bar{\bar{P}}}, \tag{26a}$$

$$2\frac{a(\alpha\bar{\bar{S}}+\gamma\bar{\bar{I}})}{\theta+\bar{\bar{P}}}(P-\bar{\bar{P}})^2+b(I-\bar{\bar{I}})^2<\frac{1}{2}\sigma_{13}+\frac{b}{2}\sigma_{12}+\frac{1}{2}\sigma_{23}, \tag{26b}$$

where $\sigma_{12}=\left[(S-\bar{\bar{S}})+(I-\bar{\bar{I}})\right]^2$, $\sigma_{13}=\left[\sqrt{b}(S-\bar{\bar{S}})+\sqrt{\frac{a(\alpha\bar{\bar{S}}+\gamma\bar{\bar{I}})}{\theta+\bar{\bar{P}}}}(P-\bar{\bar{P}})\right]^2$, and $\sigma_{23}=$

$\left[\sqrt{b}(I-\bar{\bar{I}})+\sqrt{\frac{a(\alpha\bar{\bar{S}}+\gamma\bar{\bar{I}})}{\theta+\bar{\bar{P}}}}(P-\bar{\bar{P}})\right]^2$.

Proof. Define ϑ_4 as a real valued function that is given by

$$\vartheta_4=\left(S-\bar{\bar{S}}-\bar{\bar{S}}\ln\frac{S}{\bar{\bar{S}}}\right)+\left(I-\bar{\bar{I}}-\bar{\bar{I}}\ln\frac{I}{\bar{\bar{I}}}\right)+\left(P-\bar{\bar{P}}-\bar{\bar{P}}\ln\frac{P}{\bar{\bar{P}}}\right).$$

It is clear that ϑ_4 is a positive definite function that is defined for all $\{(S,I,P)\in\mathfrak{L}: S>0, I>0, P>0\}$. Now by differentiating ϑ_4 w.r.t. time, and then simplifying the result, it is obtained that:

$$\begin{aligned}\frac{d\vartheta_4}{dt}\leq\ & -b\left(S-\bar{\bar{S}}\right)^2-b(S-\bar{\bar{S}})(I-\bar{\bar{I}})+\frac{a(\alpha\bar{\bar{S}}+\gamma\bar{\bar{I}})}{\theta+\bar{\bar{P}}}(P-\bar{\bar{P}})^2\\ & -\left[\frac{rk}{(1+kP)(1+k\bar{\bar{P}})}+a-\frac{a\alpha P}{\theta+P}\right](S-\bar{\bar{S}})(P-\bar{\bar{P}}).\\ & -\left[a-\frac{a\gamma P}{\theta+P}\right](I-\bar{\bar{I}})(P-\bar{\bar{P}})\end{aligned}$$

Further simplification gives that:

$$\begin{aligned}\frac{d\vartheta_4}{dt}<\ & -\frac{1}{2}\left[\sqrt{b}(S-\bar{\bar{S}})+\sqrt{\frac{a(\alpha\bar{\bar{S}}+\gamma\bar{\bar{I}})}{\theta+\bar{\bar{P}}}}(P-\bar{\bar{P}})\right]^2\\ & -\frac{b}{2}\left[(S-\bar{\bar{S}})+(I-\bar{\bar{I}})\right]^2+2\frac{a(\alpha\bar{\bar{S}}+\gamma\bar{\bar{I}})}{\theta+\bar{\bar{P}}}(P-\bar{\bar{P}})^2\\ & -\frac{1}{2}\left[\sqrt{b}(I-\bar{\bar{I}})+\sqrt{\frac{a(\alpha\bar{\bar{S}}+\gamma\bar{\bar{I}})}{\theta+\bar{\bar{P}}}}(P-\bar{\bar{P}})\right]^2+b(I-\bar{\bar{I}})^2.\end{aligned}$$

Therefore, the derivative $\frac{d\vartheta_4}{dt}$ is negative definite under the conditions (26a) and (26b). Moreover, since the function ϑ_4 is radially unbounded then all the solutions, which are initiated in the interior of the sub-region of $\mathfrak{L}$ and satisfy the conditions (26a), and (26b) are approached asymptotically to PEP. Hence the proof is done.

5. BIFURCATION ANALYSIS

The influence of varying the parameter value on the dynamic of the system (1) is investigated in this section. Now, in order to compute the second derivative of the J, system (1) is rewritten in the vector form as follows:

$$\frac{dX}{dT} = F(X,\varepsilon), \text{ with } X = (S,I,P)^T \text{ and } F = (Sg_1, Ig_2, Pg_3)^T \tag{27}$$

Therefore, according to the JM of the system (1) at the point (S,I,P) given by Eq. (8) it is obtained that:

$$D^2F(X,\varepsilon)(\Phi,\Phi) = [q_{i1}]_{3\times1} \tag{28}$$

where $\Phi = (v_1, v_2, v_3)^T$ and ε is any bifurcation parameter, with

$$q_{11} = -2bv_1^2 - 2(b+\beta)v_1v_2 - 2\left(\frac{rk}{(1+kP)^2} + a\right)v_1v_3 + 2\frac{rk^2S}{(1+kP)^3}\,v_3^2,$$
$$q_{21} = 2\beta v_1v_2 - 2av_2v_3,$$
$$q_{31} = 2a\alpha\left(\frac{2\theta P+P^2}{(\theta+P)^2}\right)v_1v_3 + 2a\gamma\left(\frac{2\theta P+P^2}{(\theta+P)^2}\right)v_2v_3 + 2a(\alpha S+\gamma I)\frac{\theta^2}{(\theta+P)^3}v_3^2.$$

Theorem 8. The system (1) at the AXEP undergoes a transcritical bifurcation (TB) when the parameter d_1 passes through the value $d_1{}^* = \frac{\beta r}{b}$.

Proof. The JM of the system (1) at $(E_1, d_1{}^*)$ can be represented by

$$J_1 = J(E_1, d_1{}^*) = \begin{bmatrix} -r & -\left(r+\frac{\beta r}{b}\right) & -\left(\frac{r^2k+ra}{b}\right) \\ 0 & 0 & 0 \\ 0 & 0 & -(d_2+qE) \end{bmatrix}.$$

Then the matrix J_1 has the following eigenvalues $\lambda_{11}{}^* = -r < 0$, $\lambda_{12}{}^* = 0$, and $\lambda_{13}{}^* = -(d_2+qE) < 0$. So, the AXEP is a non-hyperbolic point.

Let $\Phi_1 = (v_{11}, v_{12}, v_{13})$ be the eigenvectors corresponding to $\lambda_{12}{}^* = 0$.

Thus $J_1\Phi_1 = 0$ gives that $\Phi_1 = \left(-(1+\frac{\beta}{b})v_{12}, v_{12}, 0\right)^T$, where v_{12} is any nonzero real number. Now, let $\psi_1 = (\varphi_{11}, \varphi_{12}, \varphi_{13})^T$ represent the eigenvectors associated with the zero eigenvalues $\lambda_{12}{}^* = 0$ of $J_1{}^T$. Thus, $J_1^T\psi_1 = 0$ gives $\psi_1 = (0, \varphi_{12}, 0)^T$ where φ_{12} represents any nonzero real number.

Now, since $F_{d_1}(X, d_1) = (0, -I, 0)^T$. Hence $F_{d_1}(E_1, d_1{}^*) = (0,0,0)^T$

Therefore, $\psi_1{}^T F_{d_1}(E_1, d_1{}^*) = 0$. Hence system (1) has no saddle-node bifurcation (SNB) in view of Sotomayor theorem.

Moreover, it is observed that $\psi_1{}^T[DF_{d_1}(E_1, d_1{}^*)\Phi_1] = -\varphi_{12}v_{12} \neq 0$

Also, by using Eq. (28), it is obtained.

$$\psi_1{}^T[D^2F(E_1, d_1{}^*)(\Phi_1, \Phi_1)] = -2(1+\tfrac{\beta}{b})\,\beta\varphi_{12}v_{12}{}^2 \neq 0.$$

Then a TB occurs ear AXEP when $d_1 = d_1{}^*$, however pitchfork bifurcation (PB) can't occur. Note that, since PFEP is unconditionally LAS whenever it exists, then it is a hyperbolic point always and there is no bifurcation at that point.

Theorem 9. Assume that condition (16a) and (16b) holds, then the system (1) near DFEP undergoes a TB when the parameter β passes through the value $\beta^* = \frac{a\bar{P}+d_1}{\bar{S}}$ if the following condition is satisfied

$$\beta^*\tau_1 \neq a\tau_2 \tag{29}$$

Proof. The JM of the system (1) at (E_3, β^*) can be represented by:

$$J_2 = J(E_3, \beta^*) = \begin{bmatrix} -b\bar{S} & -(b+\beta^*)\bar{S} & -\left(\frac{rk}{(1+k\bar{P})^2}+a\right)\bar{S} \\ 0 & 0 & 0 \\ \frac{a\alpha\bar{P}^2}{\theta+\bar{P}} & \frac{a\gamma\bar{P}^2}{\theta+\bar{P}} & \frac{a\alpha\theta\bar{S}\bar{P}}{(\theta+\bar{P})^2} \end{bmatrix} = (a_{ij}).$$

Then the matrix has two eigenvalues having negative real parts due to conditions (16a)-(16b), which are given by Eq. (15b). While the third is zero. Hence it is a non-hyperbolic point.

Let $\Phi_2 = (v_{21}, v_{22}, v_{23})$ be the eigenvectors of J_2 corresponding to $\lambda_{32}{}^* = 0$. Thus $J_2\Phi_2 = 0$ gives that $\Phi_2 = (\tau_1 v_{23}, v_{23}, \tau_2 v_{23})^T$, where $\tau_1 = \frac{a_{13}a_{32}-a_{33}a_{12}}{a_{11}a_{33}-a_{13}a_{31}}$ and $\tau_2 = \frac{a_{31}a_{12}-a_{11}a_{32}}{a_{11}a_{33}-a_{13}a_{31}}$, while

v_{23} represents any nonzero real number.

Now, let $\psi_2 = (\varphi_{21}, \varphi_{22}, \varphi_{23})^T$ be the eigenvectors associated with the zero eigenvalue $\lambda_2{}^* = 0$ of $J_2{}^T$ Thus, $J_2^T\psi_2 = 0$ gives $\psi_2 = (0, \varphi_{23}, 0)^T$ where φ_{23} represents any nonzero real number.

Now, since $F_\beta(X, \beta) = (-SI, SI, 0)^T$. Hence $F_\beta(E_3, \beta^*) = (0,0,0)^T$

Therefore, $\psi_2{}^T[F_\beta(E_3, \beta^*)] = 0$. Hence system (1) has no SNB in view of the Sotomayor theorem.

Moreover, it is observed that $\psi_2{}^T[DF_\beta(E_3, \beta^*)\Phi_2] = \bar{S}\varphi_{23}v_{23} \neq 0$

Now, by using Eq. (28) with the condition (29), it is obtained.

$$\psi_2{}^T[D^2F(E_3, \beta^*)\,(\Phi_2, \Phi_2)] = 2\varphi_{23}v_{23}{}^2(\beta^*\tau_1 - a\tau_2) \neq 0.$$

Then the system (1) undergoes a TB near DFEP when $\beta = \beta^*$.

Theorem 10. Assume that the conditions (17a) and (17c) are satisfied, then the system (1) near PEP undergoes an SNB when the parameter γ passes through the value $\gamma^* = \frac{-h_{12}(h_{21}h_{33}^* - h_{23}h_{31})}{(h_{11}h_{23} - h_{13}h_{21})}\frac{\theta+\bar{\bar{P}}}{a\bar{\bar{P}}^2}$ if the following condition is satisfied.

$$\tau_5 q_{11}{}^* + \tau_6 q_{21}{}^* + q_{31}{}^* \neq 0, \tag{30}$$

where h_{ij} are given in the Eq. (18), while all the new symbols are given in the proof.

Proof. The JM of the system (1) at PEP that is given in Eq. (18), can be rewritten when $\gamma = \gamma^*$ by:

$$J_3 = J(E_4, \gamma^*)\begin{bmatrix} -b\bar{\bar{S}} & -(b+\beta)\bar{\bar{S}} & -\left(\frac{rk}{\left(1+k\bar{\bar{P}}\right)^2} + a\right)\bar{\bar{S}} \\ \beta\bar{\bar{I}} & 0 & -a\bar{\bar{I}} \\ \frac{a\alpha\bar{\bar{P}}^2}{\theta+\bar{\bar{P}}} & \frac{a\,\gamma^*\bar{\bar{P}}^2}{\theta+\bar{\bar{P}}} & \frac{\theta a(\alpha\bar{\bar{S}}+,\gamma^*\bar{\bar{I}})\bar{\bar{P}}}{\theta+\bar{\bar{P}}^2} \end{bmatrix}.$$

It is easy to verify that at $\gamma = \gamma^* > 0$, the determinant of J_3 equals zero ($\delta_3 = 0$). Hence the characteristic equation that is given in Eq. (19) has zero eigenvalue and two negative real parts eigenvalues due to conditions (17a) and (17c).

Now, let $\Phi_3 = (v_{31}, v_{32}, v_{33})$ be the eigenvectors of J_3 corresponding to $\lambda^* = 0$. Then, we will get $\Phi_3 = (\tau_3 v_{33}, \tau_4 v_{33}, v_{33})^T$, where $\tau_3 = \frac{-h_{23}}{h_{21}} > 0, \tau_4 = \frac{h_{11}h_{23} - h_{13}h_{21}}{h_{12}h_{21}} < 0$, while v_{33}

represents any nonzero real number.

Now, let $\psi_3 = (\varphi_{31}, \varphi_{32}, \varphi_{33})^T$, represent the eigenvectors associated with the zero eigenvalue $\lambda^* = 0$ of $J_3{}^T$. Thus, $J_3^T \psi_3 = 0$ gives $\psi_3 = (\tau_5 \varphi_{33}, \tau_6 \varphi_{33}, \varphi_{33})^T$ where $\tau_5 = \frac{-h_{32}^*}{h_{12}}$ and $\tau_6 = \frac{h_{11}h_{32}^* - h_{31}h_{12}}{h_{12}h_{21}}$, with φ_{33} represents any nonzero real number.

Now, since $F_\gamma(X, \gamma) = (0,0, \frac{aIP^2}{\theta+P})^T$. Hence it is obtained that $F_\gamma(E_4, \gamma^*) = (0,0, \frac{a\bar{\bar{I}}\bar{\bar{P}}^2}{\theta+\bar{\bar{P}}})^T$.

Therefore, $\psi_3{}^T [F_\gamma(E_4, \gamma^*)] = \frac{a\bar{\bar{I}}\bar{\bar{P}}^2}{\theta+\bar{\bar{P}}} \varphi_{33} \neq 0.$

Now, using Eq. (28) to compute the $D^2 F_\gamma(E_4, \gamma^*)(\Phi_3, \Phi_3)$, it is obtained:

$$q_{11}{}^* = -2b\tau_3{}^2 v_{33}{}^2 - 2(b+\beta)\tau_3\tau_4 v_{33}{}^2 - 2\left(\frac{rk}{(1+k\bar{\bar{P}})^2} + a\right)\tau_3 v_{33}{}^2 + 2\frac{rk^2\bar{\bar{S}}}{(1+k\bar{\bar{P}})^3} v_{33}{}^2.$$
$$q_{21}{}^* = 2\beta\tau_3\tau_4 v_{33}{}^2 - 2a\tau_4 v_{33}{}^2.$$
$$q_{31}{}^* = 2a\alpha\left(\frac{2\theta\bar{\bar{P}}+\bar{\bar{P}}^2}{(\theta+\bar{\bar{P}})^2}\right)\tau_3 v_{33}{}^2 + 2a\gamma^*\left(\frac{2\theta\bar{\bar{P}}+\bar{\bar{P}}^2}{(\theta+\bar{\bar{P}})^2}\right)\tau_4 v_{33}{}^2 + 2a\left(\alpha\bar{\bar{S}} + \gamma^*\bar{\bar{I}}\right)\frac{\theta^2}{(\theta+\bar{\bar{P}})^3} v_{33}{}^2.$$

Accordingly, using condition (30), it is simple to verify that:

$$\psi_3{}^T\left[D^2 F_\gamma(E_4, \gamma^*)(\Phi_3, \Phi_3)\right] = \varphi_{33}(\tau_5 q_{11}{}^* + \tau_6 q_{21}{}^* + q_{31}{}^*) \neq 0.$$

Hence, system (1) undergoes an SNB and the proof is done.

6. NUMERICAL SIMULATION

In this section, a numerical simulation has been used to verify the obtained theoretical results, and understand the impact of changing the parameter values on the system's dynamics. Therefore, system (1) is solved numerically for different sets of parameters and different sets of initial conditions using MATLAB version R2013a. Then all the obtained numerical results are presented in the form of a $3D$ phase portrait and $2D$ time series. Therefore, in order to run the simulation, the following hypothetical set of biologically feasible data is used in this section.

$$\begin{gathered} r = 6\,, K = 0.4, b = 0.1, \beta = 0.4\,, a = 0.25\,, d_1 = 0.1, \\ \alpha = 0.25\,, \gamma = 0.25, A = 2, d_2 = 0.1, q = 0.2, E = 0.5. \end{gathered} \tag{31}$$

The dynamics of the system (1) using (31) is described in Fig. (1).

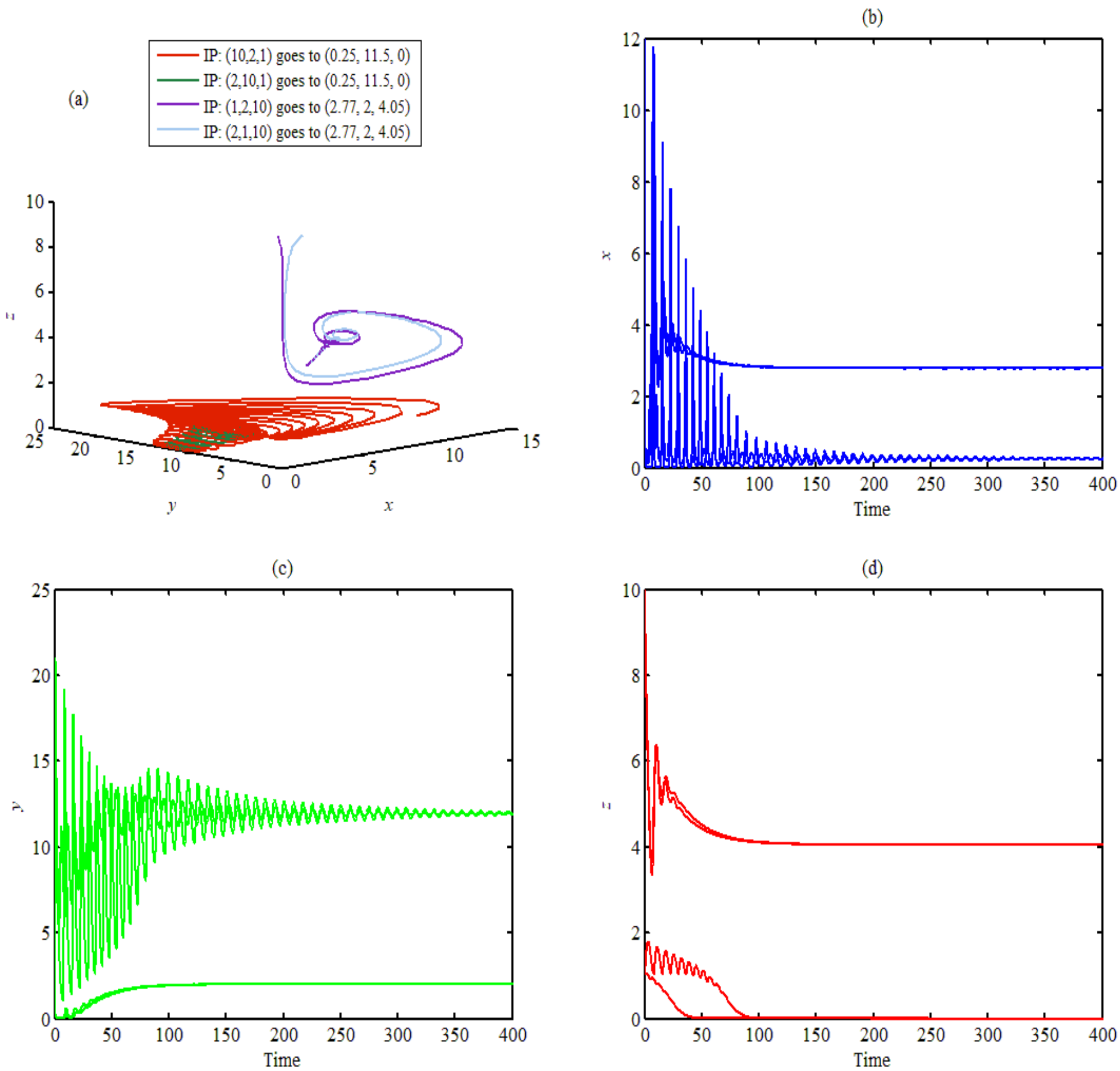

Figure 1: The solutions of the system (1) use parameters set (31) with different initial points. (a) A $3D$ phase portrait for the bi-stable case between E_2, and E_4. (b) Time series for the trajectories of x. (c) Time series for the trajectories of y. (d) Time series for the trajectories of z.

Clearly, system (1) approaches two different attractors (E_2 and E_4) using the same parameters set when the system starts from different initial points that indicate the bi-stable case. This is confirming the theoretical finding that indicates the existence of a basin of attraction for each point. Now the impact of changing the value of r is studied in Fig. (2).

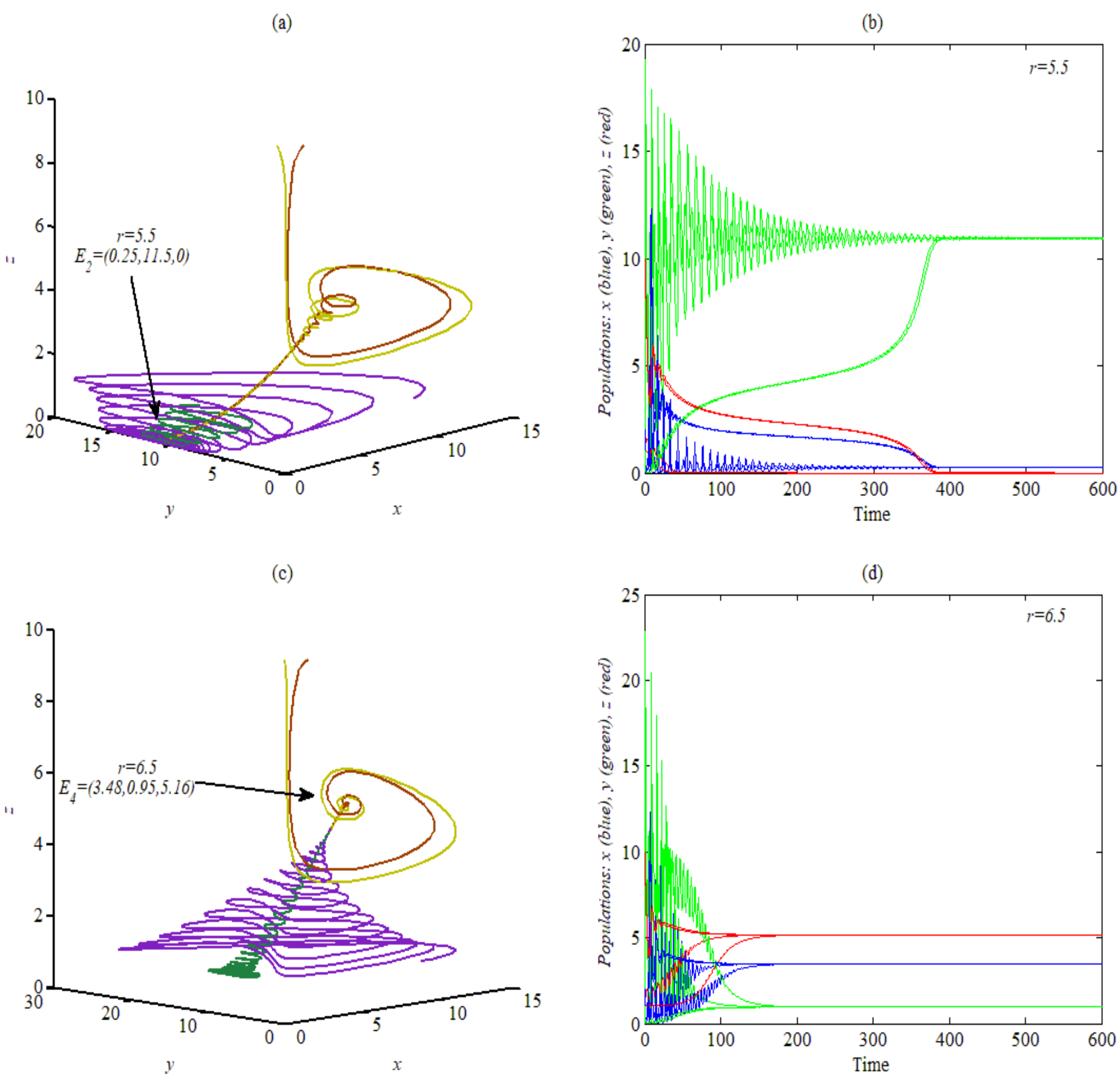

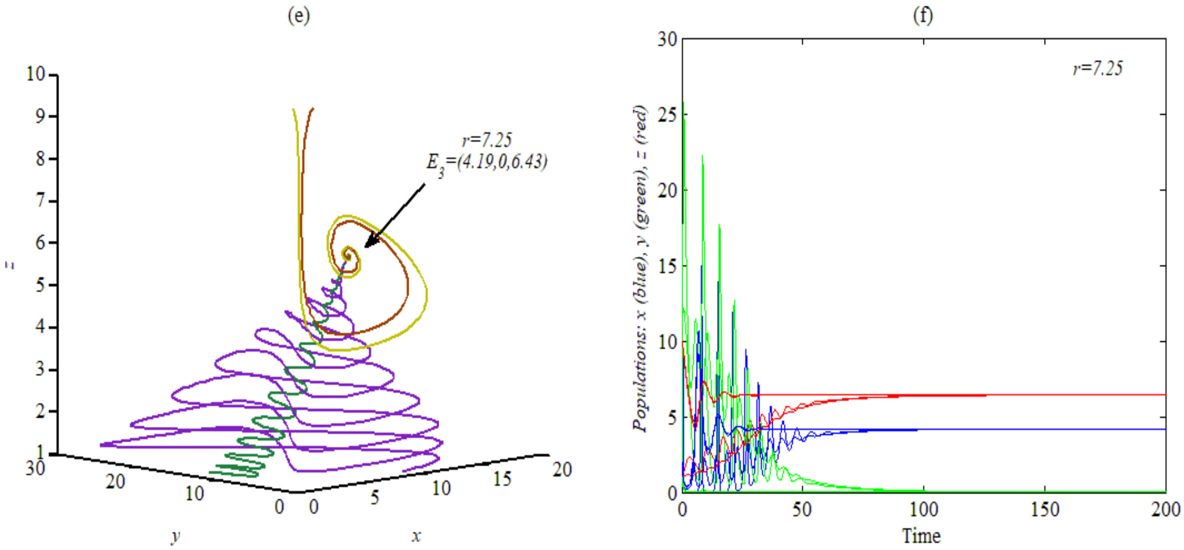

Figure 2: The solutions of the system (1) use parameters set (31) with different initial points and different values of r. (a) A $3D$ phase portrait approaches E_2 when $r = 5.5$. (b) Time series for all populations when $r = 5.5$. (c) A $3D$ phase portrait approaches E_4 when $r = 6.5$. (d) Time series for all populations when $r = 6.5$. (e) A $3D$ phase portrait approaches E_3 when $r = 7.25$. (f) Time series for all populations when $r = 7.25$.

Clearly, the range of r has different bifurcation points, and hence it affects the dynamic of the system (1). However, the impact of k on the system's dynamics is shown in Fig. (3).

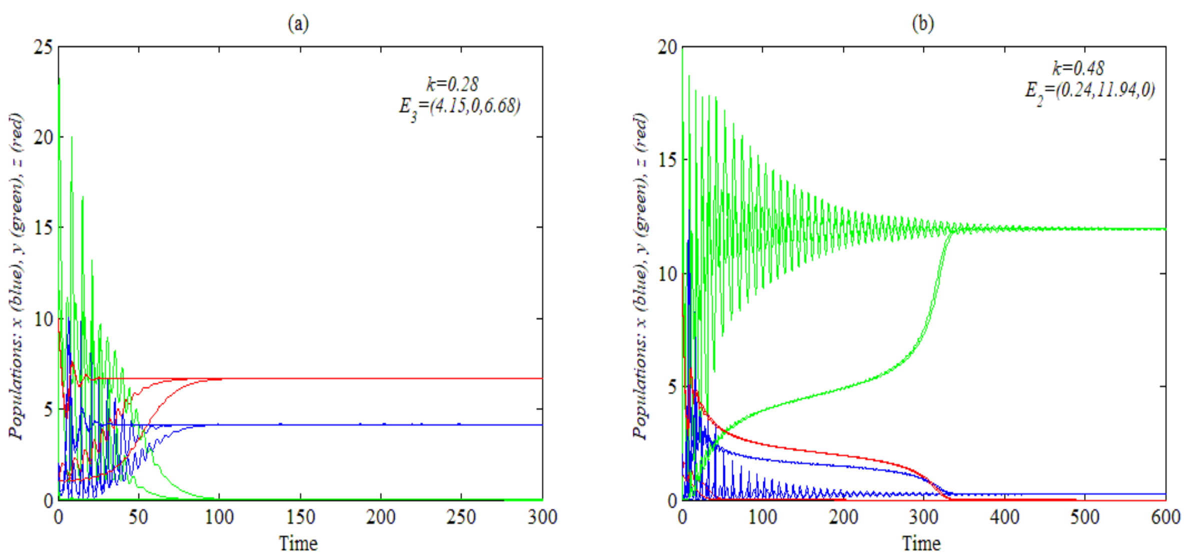

Figure 3: The solutions of the system (1) use parameters set (31) with different initial points and different values of k. (a) Time series for all populations when $k = 0.28$ that approaches E_3. (b) Time series for all populations when $k = 0.48$ that approaches E_2.

Clearly, the existence of populations depends on the value of k as shown in Fig. (3). However, the influence of changing b on the system's dynamic is shown in Fig. (4).

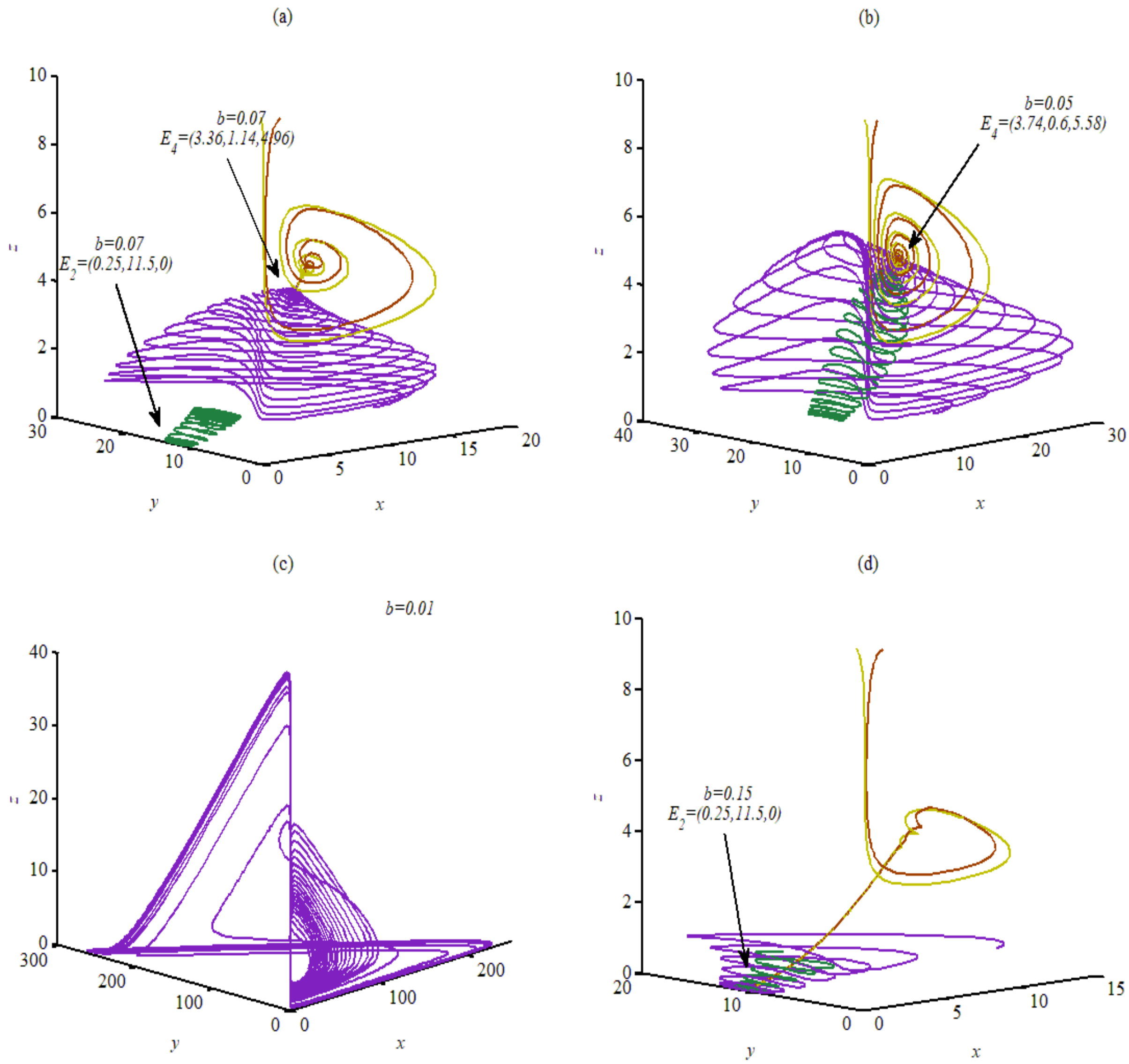

Figure 4. The solutions of the system (1) use parameters set (31) with different initial points and different values of b. (a) A $3D$ phase portrait for the bi-stable case between E_2, and E_4 when $b = 0.07$. (b) A $3D$ phase portrait approaches E_4 when $b = 0.05$. (c) A $3D$ phase portrait approaches periodic attractor when $b = 0.01$. (d) A $3D$ phase portrait approaches E_2 when $b = 0.15$.

As shown in Fig. (4), the system's dynamics are affected by the changing in b. Now, Fig. (5) shows the role of changing in β.

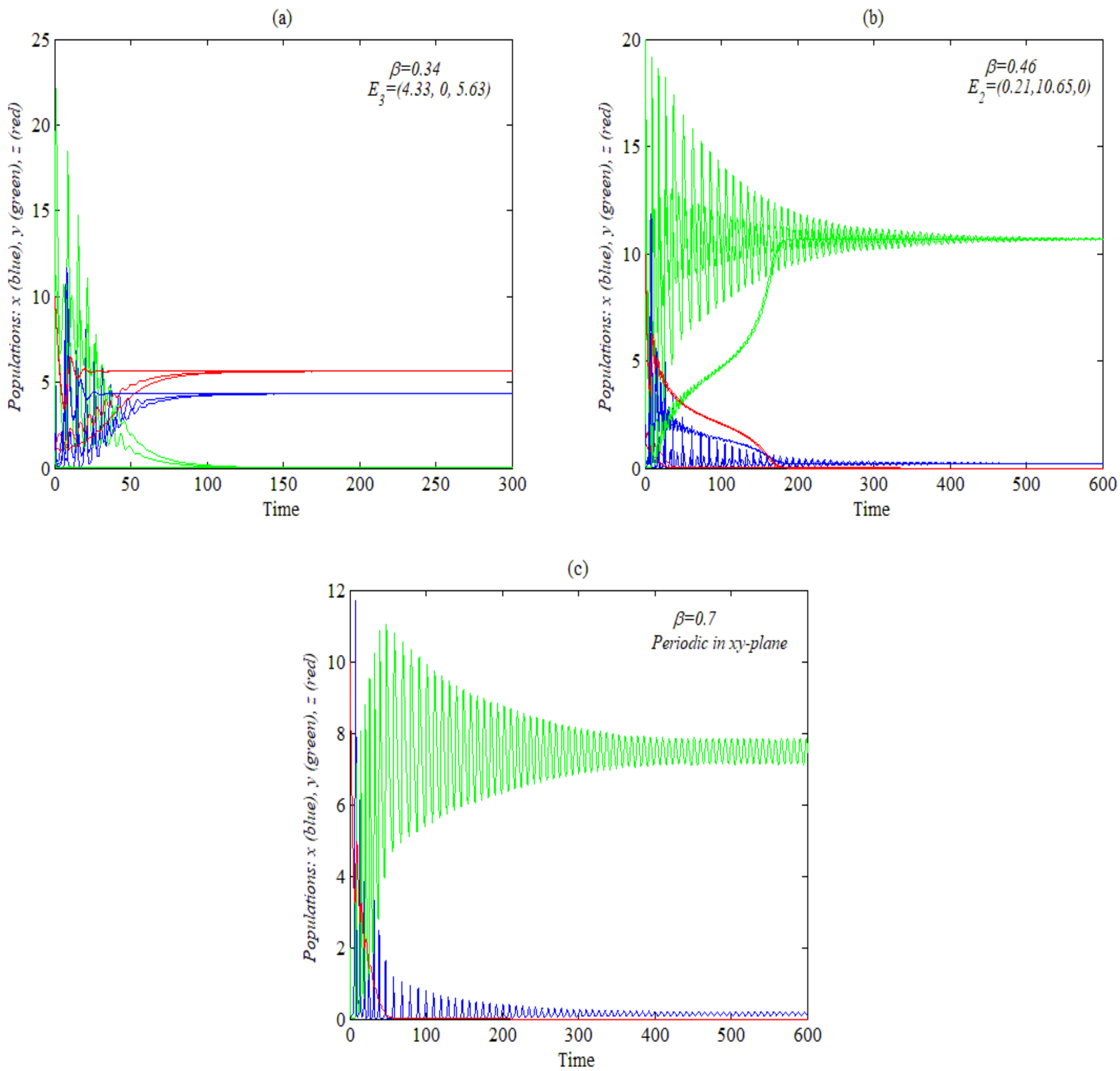

Figure 5: The solutions of the system (1) use parameters set (31) with different initial points and different values of β. (a) Time series for all populations when $\beta = 0.34$ that approaches E_3. (b) Time series for all populations when $\beta = 0.46$ that approaches E_2. (c)Time series for all populations when $\beta = 0.7$ that approaches periodic attractor in xy −plane.

It is clear from Fig. (5), that the system's dynamics are affected by the changing in β. However, Fig. (6) shows the role of changing in a.

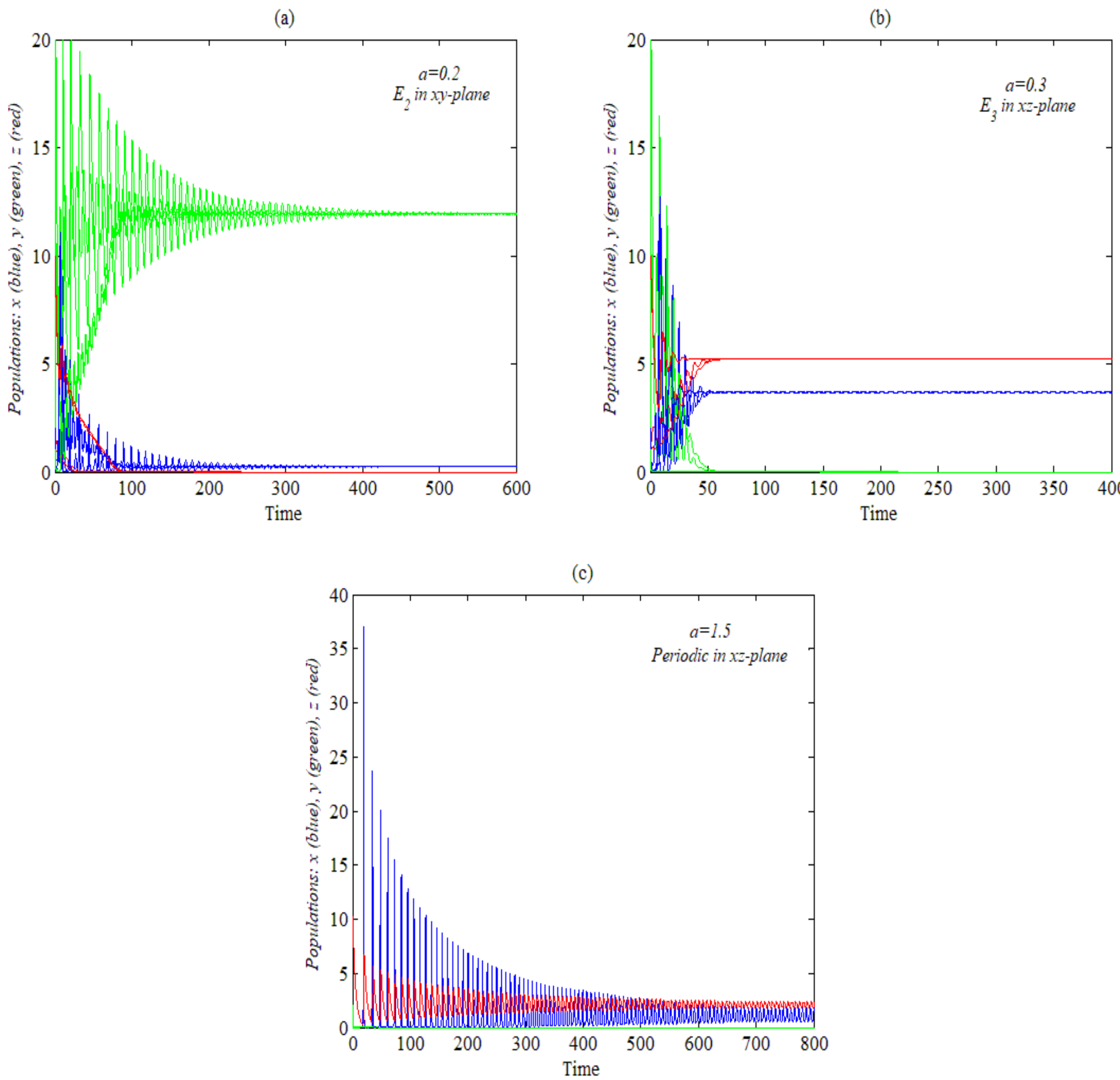

Figure 6: The solutions of the system (1) use parameters set (31) with different initial points and different values of a. (a) Time series for all populations when $a = 0.2$ that approaches E_2. (b) Time series for all populations when $a = 0.3$ that approaches E_3. (c)Time series for all populations when $a = 1.5$ that approaches periodic attractor in xz −plane.

Again the influence of changing α on the system's dynamic is clearly shown in Fig. (6). However, the changing of d_1 is studied in Fig. (7).

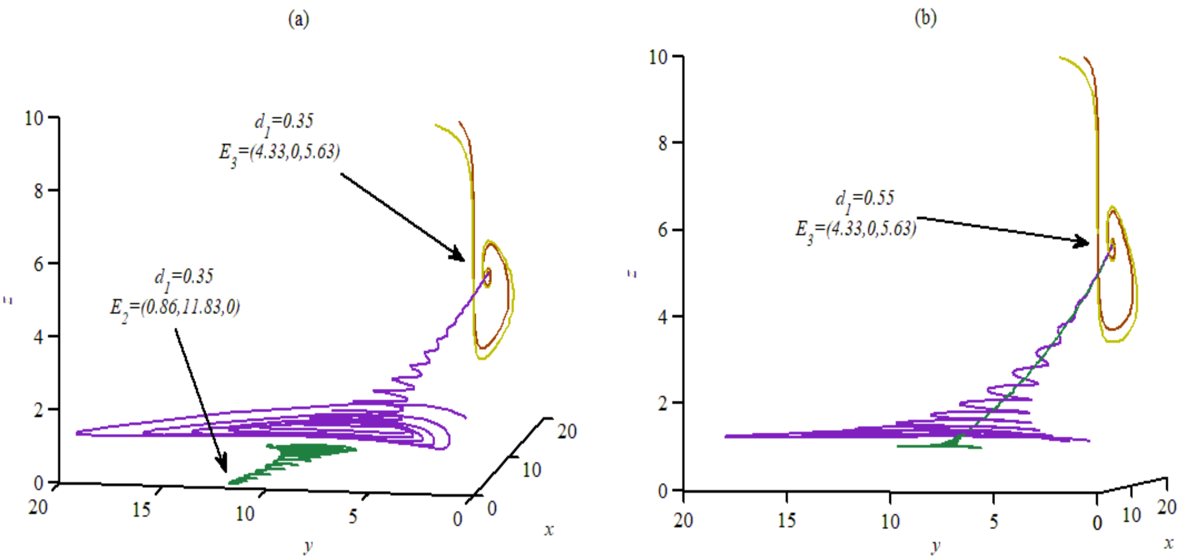

Figure 7: The solutions of the system (1) use parameters set (31) with different initial points and different values of d_1. (a) A $3D$ phase portrait for the bi-stable case between E_2, and E_3 when $d_1 = 0.35$. (b) A $3D$ phase portrait approaches E_3 when $d_1 = 0.55$.

Obviously, changing the parameter d_1 affects the system's dynamic as presented in Fig. (7). Now, the role of changing the parameter α on the system's dynamic is studied in Fig. (8).

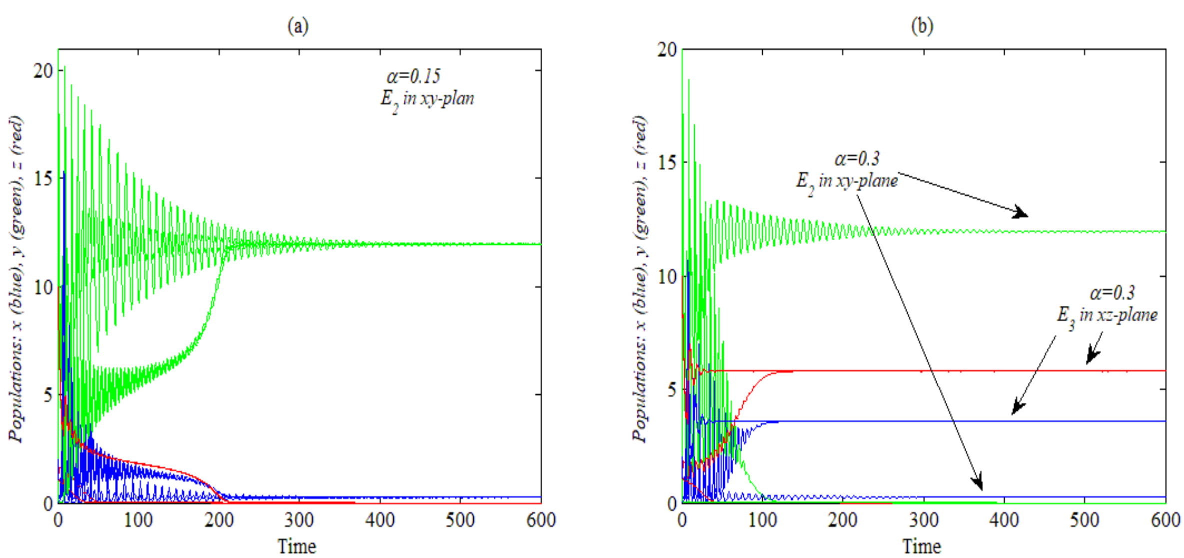

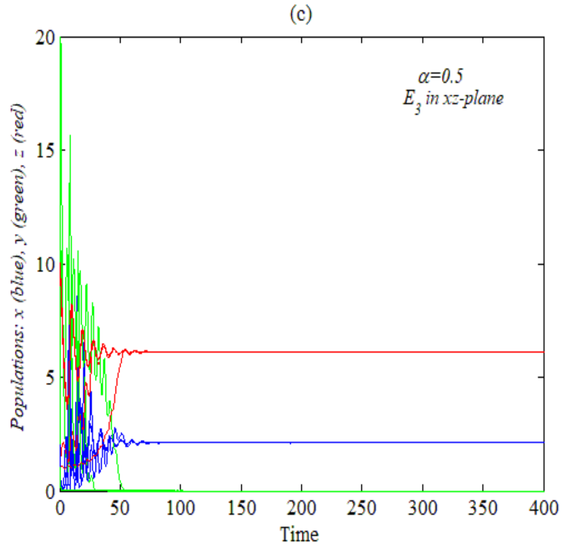

Figure 8: The solutions of the system (1) use parameters set (31) with different initial points and different values of α. (a) Time series for all populations when $\alpha = 0.15$ that approaches E_2. (b) Time series for all populations shows the bi-stable case between E_2, and E_3 when $\alpha = 0.3$.. (c) Time series for all populations when $\alpha = 0.5$ that approaches E_3.

The impact of changing the parameter α on the dynamic of the system (1) is obvious from Fig. (8). However, the change in parameter γ is investigated in Fig. (9).

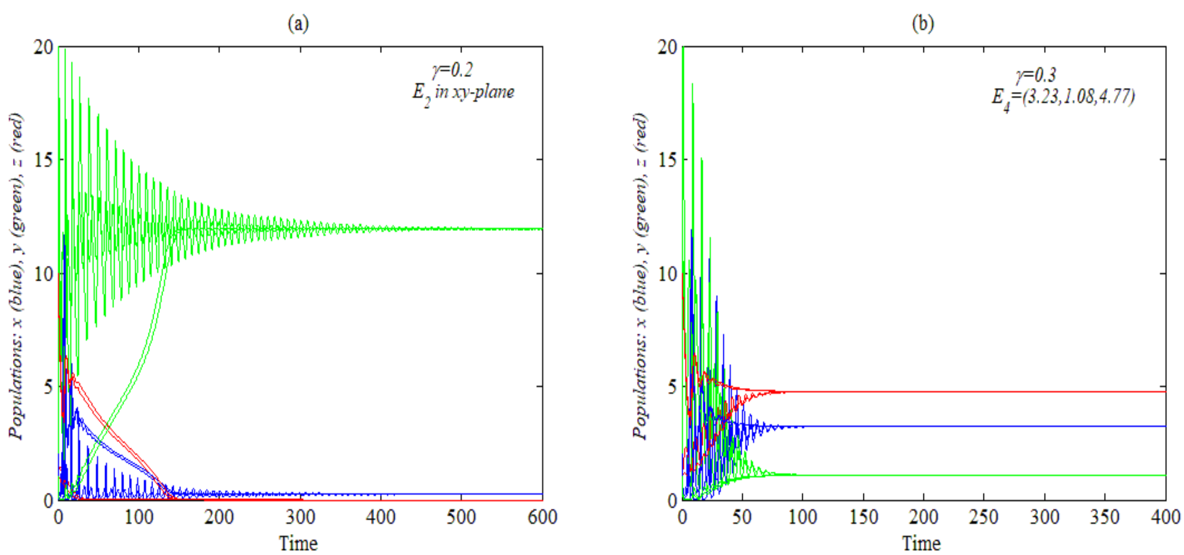

Figure 9: The solutions of the system (1) use parameters set (31) with different initial points and different values of γ. (a) Time series for all populations when $\gamma = 0.2$ that approaches E_2. (b) Time series for all populations when $\gamma = 0.3$ that approaches E_4.

Similarly, Fig. (9) clearly shows the influence of the system's dynamics due to changing in the γ. However, the influence of changing the parameters θ, and d_2 on the system's dynamic is studied in Fig. (10) and (11) respectively.

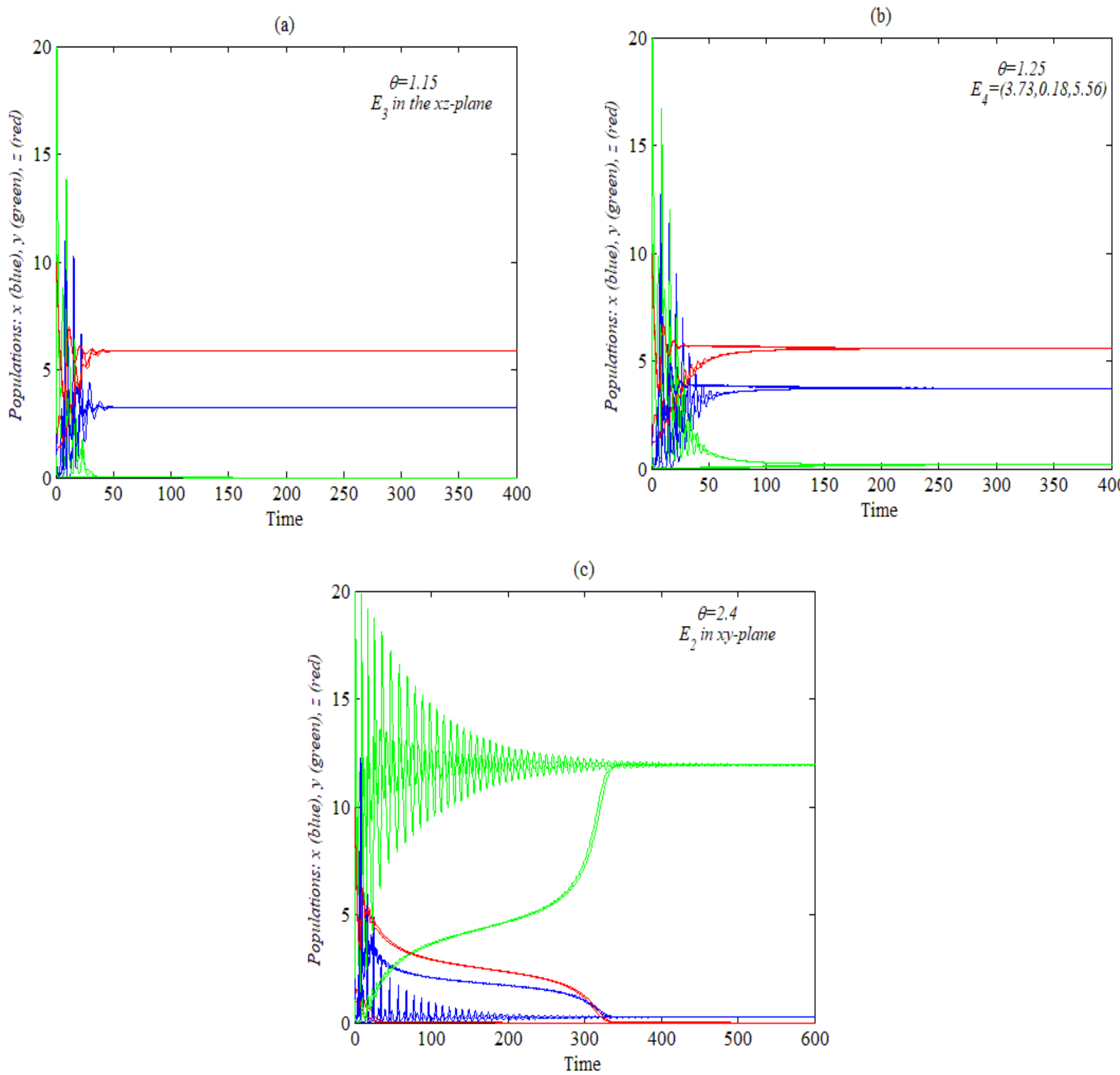

Figure 10: The solutions of the system (1) use parameters set (31) with different initial points and different values of θ. (a) Time series for all populations when $\theta = 1.15$ that approaches E_3. (b) Time series for all populations when $\theta = 1.25$ that approaches E_4. (c) Time series for all populations when $\theta = 2.4$ that approaches E_2.

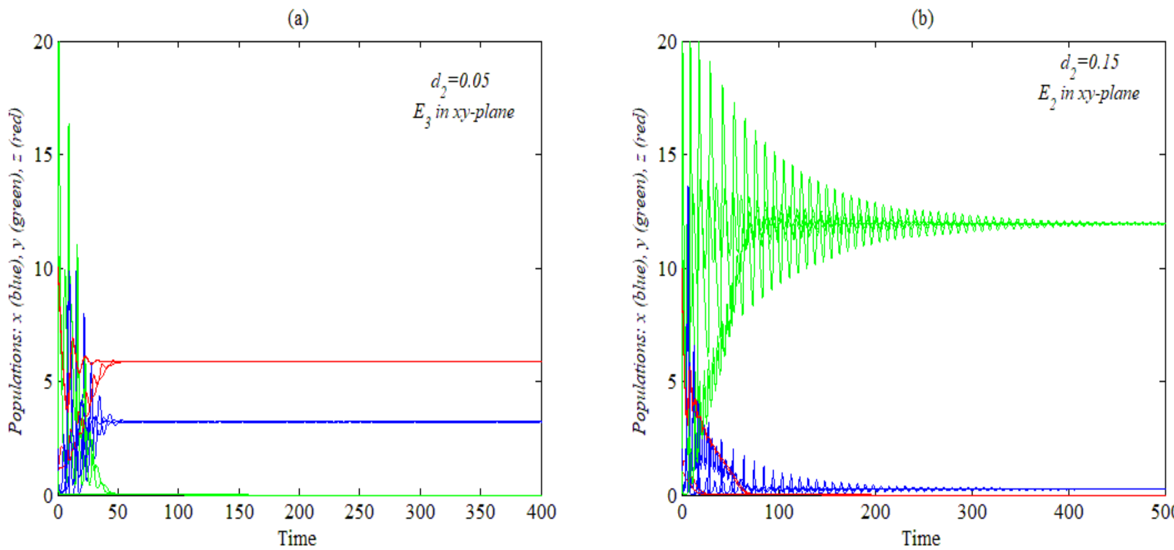

Figure 11: The solutions of the system (1) use parameters set (31) with different initial points and different values of d_2. (a) Time series for all populations when $d_2 = 0.05$ that approaches E_3. (b) Time series for all populations when $d_2 = 0.15$ that approaches E_2

Further investigation of the remaining parameters, shows that the parameters q and E have a similar influence as that shown for θ on the dynamic of the system (1).

7. Discussion and Conclusion

Predator under the effect of the weak Allee effect and harvesting is proposed and studied. The influence of fear from the predation process is considered. The solution properties of the proposed system are studied. All possible equilibrium points are determined. The stability analysis of the equilibrium points is investigated. The possible basin of attraction for each point is determined. The survival conditions of the system throughout the entire time are constructed. The impact of varying the values of the parameters on the dynamics of the system is studied using the Sotomayor theorem for local bifurcation. Numerical simulation was used to investigate the global dynamics of the proposed system and specify the parameter set that controls the dynamics of the system (1) using a hypothetical set of parameters.

Depending on the numerical results, the following observations were obtained. The system (1) undergoes a bi-stable case between the PFEP and PEP due to the fact that PFEP is unconditionally stable whenever it exists and the selected data set satisfies the existence condition. Hence whenever the initial point falls near the xy −plane there is some trajectories approach to PFEP. Decreasing the intrinsic growth rate of the prey leads to extinction in predator species and the solution approaches PFEP from different initial points. However. Increasing the value of the growth rate makes the system approaches globally to PEP for a specific range. Then extinction happens in the infected population of prey and the solution approaches DFEP. Otherwise, the system still has a bi-stable behavior. However, decreasing the fear rate causes extinction in the infected population due to the weakness of the individuals in this compartment and the high possibility of catching them by a predator. However, increasing the value of the fear rate leads to extinction in a predator species due to hiding prey that causes unavailability of food. Otherwise, the system still undergoes a bi-stable behavior.

The intraspecific competition of the prey has a clear influence on the system's dynamics so that the dynamics transfer from bi-stable to GAS at a PEP and then the system losses its stability and undergoes periodic dynamics in the interior of their state space when the intraspecific competition decrease. However, the system losses persistence and the solution goes to PFEP as the value of the intraspecific competition increase. The decreasing infection rate yields extinction of the infected population and the system approaches DFEP. On the other hand, rising the infection rate causes extinction in predator species and the solution approaches PFEP. Moreover, rising the value of the infection rate further leads to losing the stability of PFEP and periodic dynamics in the xy −plane appear. In contrast to the infection rate, lowering the attack rate leads to the extinction of predator species and hence the system approaches PFEP while rising the attack rate leads to the extinction of the infected prey and hence the system approaches DFEP. Further, increasing the attack rate makes the system lose its stability at DFEP and goes to periodic dynamics in the xz −plane.

Although decreasing the death rate of the infected prey does not change the behavior of the system (1), it is observed that rising this value leads first to the transfer of the bi-stable case between PFEP and PEP to bi-stable between PFEP and DFEP and then the system approaches asymptotically to DFEP only. On the other hand, lowering the conversion rate of the susceptible prey to the predator leads to the extinction of the predator and the system approaches PFEP, however rising their value causes extinction in infected prey and hence the system approaches DFEP. Otherwise, the system undergoes a bi-stable behavior. Also, lowering the conversion rate of the infected prey to the predator leads to the extinction of the predator, and hence the system has a GAS at PFEP. While rising the value of this parameter causes stabilizing of the system at a PEP.

The Allee effect rate has the same impact on the system's dynamics as that occurs with the infection rate when decreasing their value, so that the infected prey disappears and the solution approaches DFEP. However, increasing their value leads to the extinction in the predator species and hence the system approaches PFEP. Otherwise, the system has a bi-stable behavior case. Finally, it is observed that varying the predator death rate, the harvesting catchability constant and the effort rate has the similar influence of the system's dynamics as that shown with Allee effect rate.

According to the above, the system (1) is very sensitive to changing in their parameters and undergoes different behavior.

CONFLICT OF INTERESTS

The authors declare that there is no conflict of interests.

REFERENCES

[1] R.M. Anderson, R.M. May, Infectious diseases and population cycles of forest insects, Science. 210 (1980), 658–661. https://doi.org/10.1126/science.210.4470.658.

[2] E. Venturino, Ecoepidemiology: A more comprehensive view of population interactions, Math. Model. Nat. Phenom. 11 (2015), 49–90. https://doi.org/10.1051/mmnp/201611104.

[3] E. Beretta, Y. Kuang, Modeling and analysis of a marine bacteriophage infection, Math. Biosci. 149 (1998), 57–76. https://doi.org/10.1016/s0025-5564(97)10015-3.

[4] J. Chattopadhyay, O. Arino, A predator-prey model with disease in the prey, Nonlinear Anal., Theory Meth. Appl. 36 (1999), 747–766. https://doi.org/10.1016/s0362-546x(98)00126-6.

[5] N. Bairagi, P.K. Roy, J. Chattopadhyay, Role of infection on the stability of a predator–prey system with several response functions-A comparative study, J. Theor. Biol. 248 (2007), 10–25. https://doi.org/10.1016/j.jtbi.2007.05.005.

[6] R. Bhattacharyya, B. Mukhopadhyay, On an eco-epidemiological model with prey harvesting and predator switching: Local and global perspectives, Nonlinear Anal., Real World Appl. 11 (2010), 3824–3833. https://doi.org/10.1016/j.nonrwa.2010.02.012.

[7] B.W. Kooi, G.A.K. van Voorn, K. pada Das, Stabilization and complex dynamics in a predator–prey model with predator suffering from an infectious disease, Ecol. Complex. 8 (2011) 113–122. https://doi.org/10.1016/j.ecocom.2010.11.002.

[8] X. Liu, Bifurcation of an eco-epidemiological model with a nonlinear incidence rate, Appl. Math. Comput. 218 (2011), 2300–2309. https://doi.org/10.1016/j.amc.2011.07.050.

[9] R.K. Naji, A.N. Mustafa, The dynamics of an eco-epidemiological model with nonlinear incidence rate, J. Appl. Math. 2012 (2012), 852631. https://doi.org/10.1155/2012/852631.

[10] S. Biswas, S. Samanta, J. Chattopadhyay, A model based theoretical study on cannibalistic prey–predator system with disease in both populations, Differ. Equ. Dyn. Syst. 23 (2014), 327–370. https://doi.org/10.1007/s12591-014-0211-0.

[11] W.C. Allee, Animal aggregations: A study in general sociology, University of Chicago Press, Chicago, Illinois, (1931).

[12] M.H. Wang, M. Kot, Speeds of invasion in a model with strong or weak Allee effects, Math. Biosci. 171 (2001), 83–97. https://doi.org/10.1016/s0025-5564(01)00048-7.

[13] F. Courchamp, L. Berec, J. Gascoigne, Allee effects in ecology and conservation, Oxford University Press, Oxford, (2008).

[14] R. Burrows, H. Hofer, M. L. East, Population dynamics, intervention and survival in African wild dogs (Lycaon pictus), Proc. R. Soc. Lond. B. 262 (1995), 235–245. https://doi.org/10.1098/rspb.1995.0201.

[15] F. Courchamp, T. Clutton-Brock, B. Grenfell, Multipack dynamics and the Allee effect in the African wild dog,

Lycaon pictus, Animal Conserv. 3 (2000), 277–285. https://doi.org/10.1111/j.1469-1795.2000.tb00113.x.

[16] E. Angulo, G.W. Roemer, L. Berec, et al. Double Allee effects and extinction in the island fox, Conserv. Biol. 21 (2007), 1082–1091. https://doi.org/10.1111/j.1523-1739.2007.00721.x.

[17] D.L. Clifford, J.A.K. Mazet, E.J. Dubovi, et al. Pathogen exposure in endangered island fox (Urocyon littoralis) populations: Implications for conservation management, Biol. Conserv. 131 (2006), 230–243. https://doi.org/10.1016/j.biocon.2006.04.029.

[18] M. Su, C. Hui, Y. Zhang, Z. Li, Spatiotemporal dynamics of the epidemic transmission in a predator-prey system, Bull. Math. Biol. 70 (2008), 2195–2210. https://doi.org/10.1007/s11538-008-9340-3.

[19] H.A. Satar, The dynamics of an eco-epidemiological model with allee effect and harvesting in the predator, J. Southwest Jiaotong Univ. 55 (2020), 1-18. https://doi.org/10.35741/issn.0258-2724.55.2.29.

[20] S.K. Sasmal, J. Chattopadhyay, An eco-epidemiological system with infected prey and predator subject to the weak Allee effect, Math. Biosci. 246 (2013), 260–271. https://doi.org/10.1016/j.mbs.2013.10.005.

[21] C.W. Clark, Mathematical Bioeconomics: The optimal management of renewable resources, John Wiley & Sons, New York, (1976).

[22] M.W. Hirsch, S. Smale, Differential equations, dynamical systems, and linear algebra, Academic Press, New York, 1974.

[23] J.D. Murray, Mathematical biology, Springer-Verlag, Berlin, 1989.

[24] L. Perko, Differential equations and dynamical systems, Third Edition, Springer-Verlag, New York, 2001.

[25] T. Gard, T. Hallam, Persistence in food webs—I Lotka-Volterra food chains, Bull. Math. Biol. 41 (1979), 877–891. https://doi.org/10.1016/s0092-8240(79)80024-5.